Random laser in the localized regime

P. Sebbah and C. Vanneste
Laboratoire de Physique de la Matière Condensée, CNRS UMR 6622, Université de Nice–Sophia Antipolis, Parc Valrose, 06108, Nice Cedex 02, France

(Received 14 May 2002; published 23 October 2002)

We present detailed calculations of laser action in two-dimensional disordered systems in the localized regime. The systems are made of circular particles imbedded in an active dielectric medium, described by a population of four-level atoms. Without pumping the active medium, the existence of localized modes is studied as a function of the filling fraction and of the radius of the scattering particles. When pumping the active medium above threshold, we find that the localized modes of the passive system act as the regular modes of a conventional cavity. They are not modified by the presence of gain. By introducing local pumping of the atomic system, the spectrum of the laser emission is found to depend on the position of the pump in agreement with recent experimental results. It is shown that local pumping allows a selective excitation of individual localized modes.

DOI: 10.1103/PhysRevB.66.144202 PACS number(s): 72.15.Rn, 42.55.−f, 42.25.Dd, 42.25.Fx

I. INTRODUCTION

After the predictions by Lethokov 30 years ago,[1] much theoretical and experimental work about lasing action in scattering media has been achieved in the last decade.[2–12] Two types of random laser emission have been frequently discussed, namely, amplified spontaneous emission (ASE), often referred as to random lasing with nonresonant feedback; and ''true'' laser emission or coherent feedback lasing. Amplified spontaneous emission is expected to occur in weakly disordered media for which scattering simply increases the path length of light in the active region. Coherent feedback lasing is expected to occur in more strongly disordered media where the photon mean free path is sufficiently small to provide recurrent scattering of light. Which kind of laser emission is actually observed in experiments has been debated in the literature.[4,13,14] Most analysis to date has relied on the diffusion approximation to describe wave propagation.[1,7,8,15–20] If this approximation is appropriate to describe ASE, it becomes inadequate to describe strongly disordered media where interference effects are expected to become prominent. Recently, direct resolution of Maxwell's equations has been used to describe random lasing in such media[21–25] in order to reproduce the key aspects of the experimental observations of Cao *et al.*[11]

In this paper, which provides a more detailed description of preliminary results recently presented in Ref. 23, we investigate numerically laser action in a strongly disordered two-dimensional (2D) medium in the regime of Anderson localization. In contrast to weakly scattering systems, such a medium supports modes which are spatially localized. It raises the important question of the possible role the localized modes could play in the presence of gain, by analogy with the modes of the cavity of a conventional laser. For this purpose, we solve simultaneously Maxwell's equations and the rate equations of a four-level atomic system. Our first result is that, in the presence of gain, the lasing modes are identical to the passive localized modes of the random medium. This is in agreement with analogous calculations in one-dimensional systems by Jiang and Soukoulis.[24] The localized modes in a random laser are thus proved to be equivalent to the modes of the cavity of a classical laser. Next, by locally pumping the system, it is shown that it is possible to select individually the excited mode of the random laser. More generally, while the laser spectrum obviously depends on the intensity, it also depends on the position of the pump. This result is similar to the experimental observations of Cao *et al.*[11]

The paper is organized as follows. In Sec. II, we search for the values of parameters for which the passive 2D system of circular particles without gain supports modes that are reasonably well localized. Within the range of particle diameters and volume fractions we have investigated, frequency windows where such modes exist are identified. In Sec. III, gain is introduced by coupling Maxwell's equations to the rate equations of a four-level system. First, pumping is achieved uniformly over the whole system. In the single-mode regime, the laser mode, which is first excited just above threshold, is found to be identical to a mode of the passive system. Beats between several modes of the passive system can also be observed in the multimode regime well above threshold. Next it is shown that local pumping of the system allows individual excitation of different modes of the passive system.

II. PASSIVE MEDIUM

Before studying laser action in an active random medium in Sec. III, we begin with the characterization of the passive system without amplification. We present results demonstrating that our systems exhibit localized modes within the range of parameters that we have used. We first describe the system and the numerical method we have used to solve Maxwell's equations. Next, by studying the impulse response of the system, we show that the power spectrum exhibits peaks, which are located in a set of frequency windows that do not depend on the realization of the disorder. The location of these frequency windows in the spectrum is determined as a function of the size and the volume fraction of the particles. Eventually, we show that the peaks inside those frequency windows correspond to long-lived modes, which are spatially localized inside the system.

A. Description of the 2D random medium

The system is a 2D disordered medium of size L^2. It consists of circular particles with a radius r and optical index n_2, which are randomly distributed in a background medium of an optical index n_1. This system is equivalent to a random collection of cylinders oriented along the z axis. The surface-filling fraction of the particles is Φ. The electromagnetic field is calculated using the finite-difference time-domain (FDTD) method[26] to solve Maxwell's equations. We have used PML (perfectly matched layer) absorbing conditions[27] in order to model an open system. Such absorbing conditions are very efficient to absorb the waves that leave the system. They prevent from spurious reflections at the boundaries, which otherwise would play the role of an artificial numerical cavity and would alter the lasing action described in Sec. III.[28]

We have considered a 2D transverse magnetic (TM) field. Hence Maxwell's equations read

$$\mu_0 \partial H_x/\partial t = -\partial E_z/\partial y, \tag{1a}$$

$$\mu_0 \partial H_y/\partial t = \partial E_z/\partial x, \tag{1b}$$

$$\varepsilon_i \varepsilon_0 \partial E_z/\partial t = \partial H_y/\partial x - \partial H_x/\partial y, \tag{1c}$$

where ε_0 and μ_0 are the electric permittivity and the magnetic permeability of vacuum respectively and $\varepsilon_i = n_i^2$, $i = 1,2$. In order to approach the localized regime, a large optical index contrast has been chosen, namely $n_1 = 1$ and $n_2 = 2$. Using a space increment $\Delta x = \Delta y = 10$ nm, the time increment has been chosen to be $\Delta t = \Delta x/c\sqrt{2} \approx 3.6 \times 10^{-17}$ s, where c is the speed of light in vacuum. First, such values ensure the stability of the FDTD algorithm. They are also sufficiently small compared to the optical wavelengths $\lambda \approx 500$ nm and optical periods $T \approx 1.5 \times 10^{-15}$ s considered in the following. The total size of the system has been chosen equal to $550 \times \Delta x$, which corresponds to $L = 5.5$ μm.

To study the passive modes of the system, two different sources have been used. The first source is a short electromagnetic pulse, which is injected inside the system. The response is recorded at several locations and Fourier transformed in order to obtain the power spectrum. The second source is monochromatic at an eigenfrequency selected in the power spectrum in order to excite only the corresponding eigenmode.

B. Pulse excitation and spectrum

In a first sequence of numerical experiments, a Gaussian pulse of arbitrary amplitude and of duration about 10^{-16} s is launched inside the system. The impulse response is recorded during a time window of length T_w at several nodes regularly positioned in the system. Typically, T_w has been chosen equal to about 250000 time steps (≈ 6 ps), though longer time windows have been used when necessary. Since the system is open, most of the energy of the pulse leaves the system very quickly. Hence only the signals recorded in the time window $[T_w/2, T_w]$ have been considered in order to observe the modes that have the longest lifetimes. To obtain the power spectrum, signals that are recorded at many different locations are summed before being Fourier transformed. This procedure has been chosen in order to detect all the modes, in particular the modes, which could be strongly localized in a small part of the system.

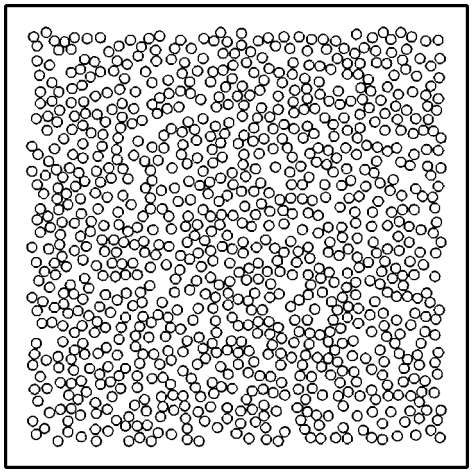

FIG. 1. An example of the random realization of circular particles: $L = 5.5$ μm, $r = 60$ nm, and $\Phi = 40\%$.

Several values of the radius r of the particles, ranging from 30 to 120 nm, as well as several values of the filling fraction Φ, ranging from 30% to 50% have been considered. For each couple (r, Φ), several realizations of the disorder (about ten) have been studied. An example of realization with $r = 60$ nm and $\Phi = 40\%$ is shown in Fig. 1. The corresponding power spectrum is shown in Fig. 2(a) (note the vertical logarithmic scale). One observes that the peaks, which correspond to the modes that have the largest lifetimes, are grouped in distinct frequency windows. Though the frequency position of individual peaks does depend on the realization of the disorder, a noticeable feature of such a spectrum is that the frequency windows themselves do not. Such windows are characteristic of all spectra corresponding

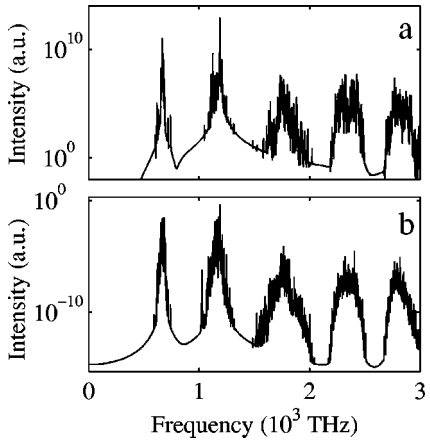

FIG. 2. (a) Power spectrum of the impulse response of the system displayed in Fig. 1. Note the logarithmic vertical scale. (b) Average of the power spectra performed over 13 different realizations of systems similar to Fig. 1.

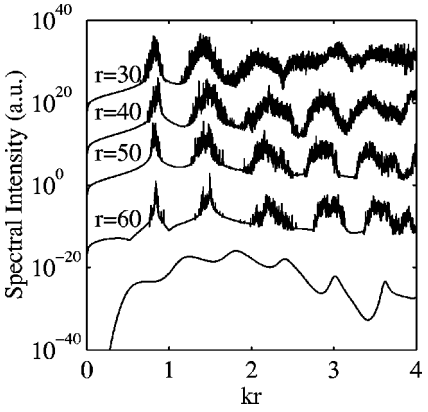

FIG. 3. Power spectra corresponding to realizations of particles with increasing radii $r=30$, 40, 50, and 60 nm at a constant filling fraction $\Phi=40\%$ as a function of $kr=2\pi r/\lambda$. The bottom curve is the Mie scattering cross section of a TM wave incident upon a cylinder with index contrast $n_2/n_1=2$. For clarity, the different curves have been shifted vertically. The intensity scale is arbitrary, but the logarithmic scale shows that the peaks are several orders of magnitude higher that the background spectrum.

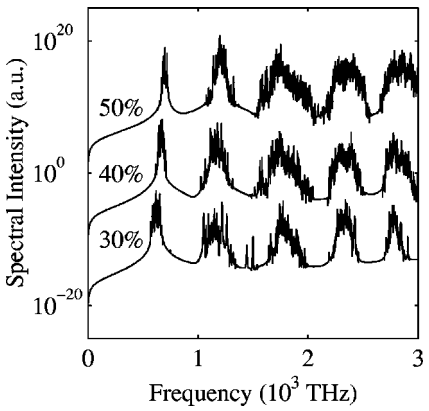

FIG. 4. Power spectra corresponding to realizations of particles of radius $r=60$ nm with increasing filling fractions $\Phi=30\%$, 40%, and 50%. For clarity, the different curves have been shifted vertically. The intensity scale is arbitrary but the logarithmic scale shows that the peaks are several orders of magnitude higher that the background spectrum.

to the same couple (r,Φ). This property is illustrated in Fig. 2(b) where spectra of 13 different random configurations corresponding to $r=60$ nm and $\Phi=40\%$ have been averaged. The resulting plot shows that the frequency windows that are observed in the spectrum of a single realization are indeed shared by the 12 other realizations. As shown in Sec. II C, the peaks in these frequency windows correspond to eigenmodes, which are spatially localized in the system.

Let us examine how the location of the frequency windows depends on r and Φ separately. First, one observes that the frequency windows shift toward higher frequencies when the radius r of the particles decreases at constant filling fraction Φ. This effect is expected since, for a given value of the filling fraction, there is only one control parameter, namely, the ratio r/λ. This is illustrated in Fig. 3, which displays the spectra of several configurations of particles with different values of r as a function of $kr=2\pi r/\lambda$ $(\Phi=40\%)$. Indeed, the positions of the frequency windows depend only on r/λ. Focusing on the curve $r=30$ nm in Fig. 3, one observes that the windows deteriorate at high frequencies. This effect is expected since, at high frequencies, λ becomes comparable to the space increment of the grid. While such a numerical limitation has been observed at sufficiently high frequencies for all values of r, it is more pronounced for small values of r. As stated above, we have used sufficiently large values of r and λ in the remaining of this work, to avoid these effects due to the numerical grid.

One can wonder whether the positions of the above frequency windows are related to the Mie resonances of a single cylinder. To answer this question, the scattering cross-section of a TM wave incident on a dielectric cylinder of index $n_2=2$ embedded in a medium of index $n_1=1$ has also been displayed in Fig. 3. One observes that the first frequency windows are clearly located between the Mie resonances. Considering, as shown later, that the frequency windows correspond to localized modes, one concludes that the localization windows do not coincide with the maxima of the scattering cross section as opposed to what one might expect.[29] This conclusion is in agreement with recent results for acoustic waves[30] and microwaves,[31] where localization was found to occur in narrow frequency windows above the Mie resonances. Our results also agree with those of Sigalas *et al.*,[32] who numerically studied two-dimensional arrays of cylinders similar to ours but with higher index contrasts.

Next, the frequency windows are found to shift toward higher frequencies when the filling fraction increases at a fixed value of the radius of the particles. This result is illustrated in Fig. 4 where the frequency windows are displayed for $r=60$ nm and different values of Φ. However, the frequency shift is small and only visible for the low frequency windows. At higher frequencies, the shift, if it still exists, is masked by the large dispersion of the widths of the windows. The same behavior has also been observed for the other values of r we have studied, namely, $r=30$, 40, and 50 nm.

C. Monochromatic excitation and eigenmodes

Let us now study the nature of the modes corresponding to the spectra described in the preceding section. Although we could have considered other values as well, from now on we will limit ourselves to $r=60$ nm and $\Phi=40\%$. The corresponding spectrum exhibits a frequency window of modes at about 6.5×10^{14} Hz, which corresponds to $\lambda\approx450$ nm (Fig. 2). This value is comparable with the values reported in recent experimental work.[11,14] Figure 5 displays an enlargement of this frequency window where well separated peaks can be identified. Three spectra have been represented, which correspond to the Fourier transform of the first, second, and third fractions of the time record of the field from 0 to T_w. The three spectra are different because the system is open and only supports leaky modes. The most leaky modes observed in the first spectrum are strongly attenuated in the second and third spectra, where only the modes with the longest lifetimes survive.

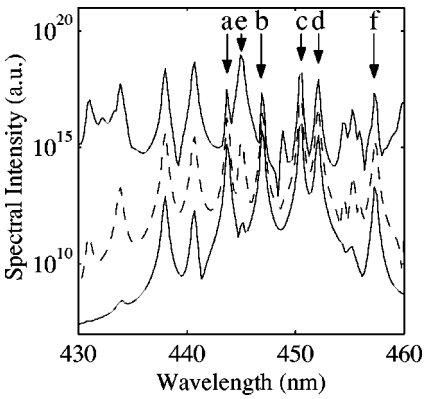

FIG. 5. Power spectra corresponding from top to bottom to three successive time records for the same system. The wavelength range corresponds to the first frequency window ($\nu \approx 0.65$ THz) of the power spectrum displayed in Fig. 2.

The modes are then excited separately by a monochromatic source at the eigenfrequencies measured in the spectrum. The monochromatic source has a Gaussian envelope of a duration larger than the inverse of the level spacing between two neighboring modes such that each mode is excited individually. Figure 6 shows the spatial maps of such excited eigenmodes after the monochromatic source has stopped. Modes *a*, *b*, *c*, and *d* are associated with the highest peaks of the third spectrum in Fig. 5 at $\lambda = 443.7$, 446.9, 450.6, and 452.1 nm, respectively. They correspond to the longest-lived modes of the system, as indicated by the small decrease of their peaks from the first to the second and third spectrum in Fig. 5. Modes *e* and *f*, at $\lambda = 445.0$ and 457.2 nm, respectively, correspond to peaks which decrease faster in Fig. 5. They are examples of modes which experience a stronger leakage through the boundaries of the system. Besides their complex shapes and random locations in the system, these modes display a strong spatial localization. Figure 7 displays a section of mode *b* along a straight line in a semilogarithmic representation. In spite of strong local fluctuations, one observes an exponential decay of the envelope whose characteristic length corresponds to the localization length ξ. For mode *b*, one finds $\xi \approx 0.5$ μm. This value is about ten times smaller than the size $L = 5.5$ μm of the system. Similar exponential decays of the envelopes have also been observed for the other modes with values of the decay length ranging from 0.5 to 1 μm. For a given mode, such values can also fluctuate in this range as a function of the orientation of the section. This behavior is not really surprising since we are considering specific realizations of disorder and modes, rather than averaged quantities.

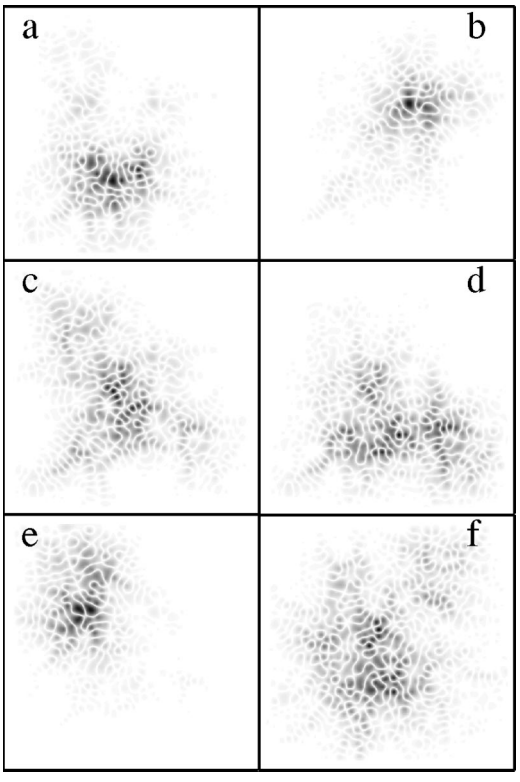

FIG. 6. Spatial distribution of the field amplitude of six localized modes corresponding to peaks *a* to *f* of Fig. 5. (a) Mode *a* ($\lambda = 443.7$ nm), (b) mode *b* ($\lambda = 446.9$ nm), (c) mode *c* ($\lambda = 450.6$ nm), (d) mode *d* ($\lambda = 452.1$ nm), (e) mode *e* ($\lambda = 445.0$ nm), and (f) mode *f* ($\lambda = 457.2$ nm).

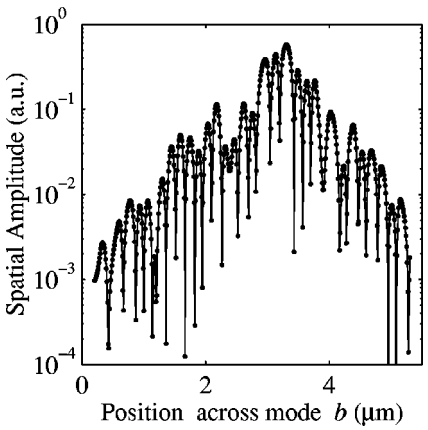

FIG. 7. Section of mode *b* in a semilogarithmic representation.

As stated above, since the system is open, it supports only leaky modes. In other words, the localized modes we have just described are not true stationary solutions of the system but exhibit losses through the boundaries. By recording the field at one location in the system, it is possible to measure the decay of an excited mode when the monochromatic source has stopped. An example of such a record is shown in Fig. 8 for mode *a*. Accurate measurements of the decay times from records similar to Fig. 8 gives values ranging from $\tau = 3.49$ ps for mode *b* to $\tau = 0.72$ ps for mode *e*. Such values correspond to quality factors $\nu/\delta\nu$ ranging from 14700 to 3030, where $\delta\nu = \tau^{-1}$ is the linewidth. These long lifetimes confirm that the corresponding modes are sufficiently well located inside the system to suffer a rather small leakage through the boundaries.

Eventually, we have checked that modes, which are strongly localized inside the system are independent of boundary conditions. Indeed, we have found that such modes are not affected when substituting the PML absorbing conditions by reflective boundary conditions. This test confirms

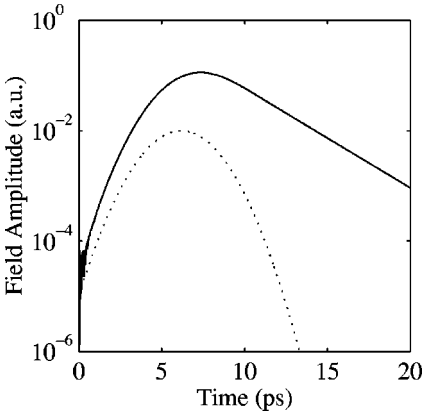

FIG. 8. Semilogarithmic representation of the field amplitude of mode *a* as a function of time, recorded at an arbitrary location in the system. The dotted line represents the amplitude of the monochromatic source. From the slope of the decaying part of the record after the end of the monochromatic source at $t \approx 12$ ps, one deduces the decay time $\tau \approx 2.41$ ps.

that the regime of Anderson localization has been reached within the limited dimensions of our systems.

To summarize the main results of this section, we have identified a range of parameters for which the passive systems that we have considered support modes that are reasonably well localized. These quasimodes exhibit long enough lifetimes so that the systems can be viewed as made of random cavities produced by the disorder. The relevance of this picture will be confirmed in Sec. III, where it is shown that these random cavities act exactly in the same way as the cavity of a classical laser when gain is introduced in the medium.

III. ACTIVE MEDIUM

A. Laser equations

The background medium of index n_1 is chosen as the active part of the system, in order to control the randomness and the gain independently. This active medium, modeled as a four-level atomic system, induces a polarization term in Maxwell's equations (1), which become

$$\mu_0 \partial H_x/\partial t = -\partial E_z/\partial y, \tag{2a}$$

$$\mu_0 \partial H_y/\partial t = \partial E_z/\partial x, \tag{2b}$$

$$\varepsilon_i \varepsilon_0 \partial E_z/\partial t + \partial P/\partial t = \partial H_y/\partial x - \partial H_x/\partial y, \tag{2c}$$

where P is the polarization density.

The time evolution of the four-level atomic system is described by conventional rate equations. The electrons in the ground level 1 are transferred to the upper level 4 by an external pump at a fixed rate W_p. Electrons in level 4 flow downward to level 3 by means of nonradiative decay processes with a characteristic time τ_{43}. This time is very short so that the electrons excited in level 4 quickly populate level 3. The intermediate levels 3 and 2 are the upper and lower levels of the laser transition, respectively. The decay rates downward from these two levels are $1/\tau_{32}$ and $1/\tau_{21}$, respectively. Moreover, stimulated transitions due to the electromagnetic field take place between these two levels. The corresponding equations have the following forms:[33]

TABLE I. Random system of particles.

Volume fraction of particles	$\Phi = 40\%$
Radius of the particles	$r = 60$ nm
Optical index of the particles	$n_2 = 2$
Optical index of the background medium	$n_1 = 1$

$$dN_1/dt = N_2/\tau_{21} - W_p N_1 \tag{3a}$$

$$dN_2/dt = N_3/\tau_{32} - N_2/\tau_{21} - (E_z/\hbar\omega_l) dP/dt \tag{3b}$$

$$dN_3/dt = N_4/\tau_{43} - N_3/\tau_{32} + (E_z/\hbar\omega_l) dP/dt \tag{3c}$$

$$dN_4/dt = -N_4/\tau_{43} + W_p N_1, \tag{3d}$$

where N_i is the population density in level i, $i = 1$ to 4. The stimulated transition rate is given by the term $(E_z/\hbar\omega_l) dP/dt$ where $\omega_l = (E_3 - E_2)/\hbar$ is the transition frequency between levels 2 and 3. Of course, E_z, P, and N_i depend on time t but also on the position $\vec{r}$ in the system.

Eventually, the polarization is described as obeying the equation[33]

$$d^2P/dt^2 + \Delta\omega_l dP/dt + \omega_l^2 P = \kappa \Delta N E_z, \tag{4}$$

where $\Delta N = N_2 - N_3$ is the population difference density between the populations in the lower and upper levels of the atomic transition. Amplification takes place when the external pumping mechanism produces population inversion, $\Delta N < 0$. The linewidth of the atomic transition is $\Delta\omega_l = 1/\tau_{32} + 2/T_2$ where the collision time T_2 is usually much smaller than the lifetime τ_{32}. The constant κ is given by $\kappa = 6\pi\epsilon_0 c^3/\omega_l^2 \tau_{32}$.

At this stage, it is useful to compare the above model to similar models introduced in the literature. Though many models of active random media have used a phenomenological negative absorption to describe the gain mechanism,[3,7,14] rate equations of atomic populations are more appropriate to understand the time evolution of such systems.[6,8,15–20] This is especially true concerning the mode competition that takes place in the multimode regime of laser systems. For instance, John and Pang[15] used a rather detailed description of the energy levels of the rhodamine 640 dye molecule in order to explain the bichromatic emission that is experimentally observed in suspensions containing that molecule.[4] However, as the regime of localization was not considered in those studies, light propagation was described in the diffusion approximation. Jiang and Soukoulis[22] were the first to couple Maxwell's equations with the rate equations of an atomic system in order to study the interplay of laser gain and Anderson localization. Our equations above are identical to those they used, except that we are now considering a two-dimensional system rather than a one-dimensional system.

The values of the different parameters that have been used in the following numerical simulations are listed in Tables I

TABLE II. Four-level atomic system.

Total atomic density	$N_T = 3.313 \times 10^{24} \mathrm{m}^{-3}$
Frequency of the atomic transition	$\nu_l = \omega_l / 2\pi = 6.71 \times 10^{14}$ Hz ($\lambda = 446.9$ nm)
Lifetime of level 4	$\tau_{43} = 10^{-13}$ s
Lifetime of level 3	$\tau_{32} = 10^{-10}$ s
Lifetime of level 2	$\tau_{21} = 5 \times 10^{-12}$ s
Collision time	$T_2 = 2 \times 10^{-14}$ s

and II. These values are close to those of dye molecules such as rhodamine 640, which has been used in several experiments. Such dye molecules exhibit short lifetimes. Numerically, this is an advantage since lifetimes of the order of 10^{-6}–10^{-3} s as encountered in many laser materials, would have been out of range of our computing capabilities. Our values have even been chosen a little bit shorter in order to reduce the computation times that are needed to achieve stationary states. However, care has been taken to maintain a good separation of the time scales associated to the different relaxation processes. With such a choice, times span the total range from the time increment $\Delta t = 2.8 \times 10^{-17}$ s to the longest time $\tau_{32} = 10^{-10}$ s. Let us recall that the decay times of the localized modes are of the order of 10^{-12} s. This value is much shorter than the lifetime τ_{32} of the upper level of the atomic transition. This situation is known to lead to the observation of spiking or relaxation oscillations when a laser is first turned on.[33,34] We shall see later that, in this respect as in many others, the random laser behaves as a conventional laser.

B. Uniform gain

1. Single-mode regime

In this section, gain is introduced by pumping the four-level atoms uniformly over the whole system. We set the pumping rate just above threshold of laser action in order to excite a single mode. Just above threshold, a stationary regime is reached after a transient exponential growth of the field amplitude (Fig. 9). On purpose, we have chosen the center frequency ν_l of the atomic transition equal to the eigenfrequency ν_b of the mode labeled *b* in Fig. 5. Hence, since this mode exhibits the longest lifetime, we expect that it will be the first mode to be excited just above threshold. Indeed, the corresponding map of the field amplitude displayed in Fig. 10 is identical to the map of mode *b*, which is displayed in Fig. 6. A more quantitative comparison indicates that the two maps are identical to a very good precision in all regions where the field amplitudes are above 1% of their maximum value. The resulting spectrum exhibits a unique peak at $\lambda = 446.9$ nm [Fig. 11(a)], which corresponds to the frequency of mode *b* (Fig. 5). This result stresses the fact that the lasing mode of a random laser is identical to the passive mode of the corresponding random medium.

2. Multimode regime

At higher pump levels, the laser emission becomes multimode. After a transient regime lasting a few picoseconds, the field becomes stationary on the average though exhibiting beats between several excited modes (Fig. 12). The field map at a particular time is shown in the inset of Fig. 12. One clearly recognizes a mixture of patterns, including modes *a*, *b*, and *e* of Fig. 6. The corresponding spectrum is shown in Fig. 13. Aside from a small pulling effect whose relative frequency shift is less than 5×10^{-4}, the high narrow peaks correspond to the eigenfrequencies of the passive system. These results confirm that the laser field corresponds to a superposition of modes of the passive system. They also agree with those of Jiang and Soukoulis,[24] who found that the shape of the wave function of a random one-dimensional system remains unchanged as gain is introduced.

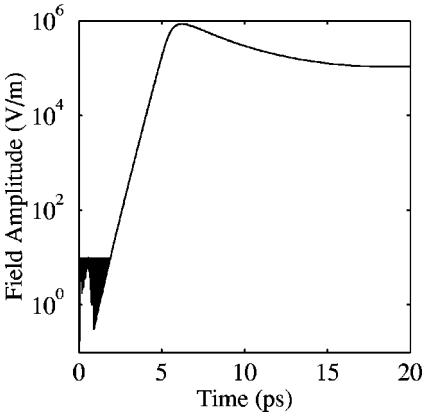

FIG. 9. Semilogarithmic representation of the field amplitude as a function of time recorded at an arbitrary location in the system, during the growth of the laser emission just above threshold. The dark area at the beginning of the record corresponds to the initial noise when the field amplitude is not yet well defined.

C. Localized gain

By adjusting the pumping rate just above threshold, we have showed in Sec. III B that one individual localized mode could be selected by the laser gain. This result was achieved by tuning the center frequency ν_l of the atomic transition to the eigenfrequency of one localized mode, namely, mode *b*.

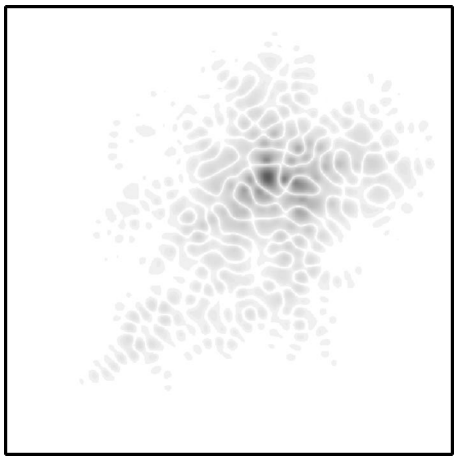

FIG. 10. Spatial distribution of the field amplitude of the laser emission just above threshold.

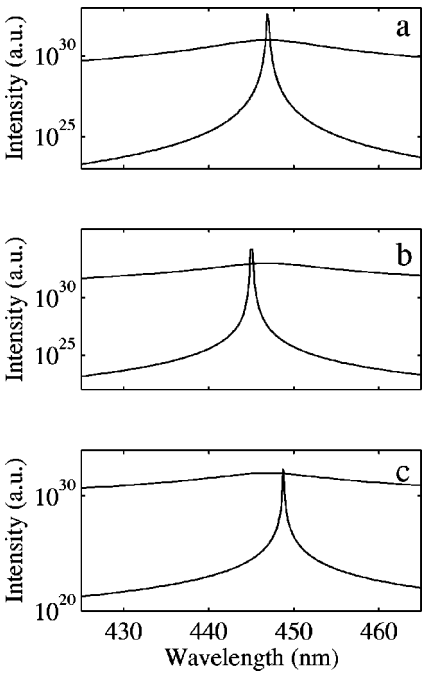

FIG. 11. Power spectrum of the laser field (a) for extended gain just above threshold, corresponding to the spatial map displayed in Fig. 10, (b) for spatially localized gain corresponding to the spatial map displayed in Fig. 15, and (c) for gain spatially localized near the boundaries and corresponding to the spatial map displayed in Fig. 17. The Lorentzian line shape of the gain is also shown. Note the logarithmic intensity scale.

The issue we consider now is to excite individually other modes. The first obvious method is to adjust the center frequency ν_l to the eigenfrequency of another mode.[24] Though achievable in numerical calculations, the gain curve is fixed by the choice of the active material, and usually cannot be adjusted in actual experiments. In fact, there exists another way to select modes individually that takes advantage of the

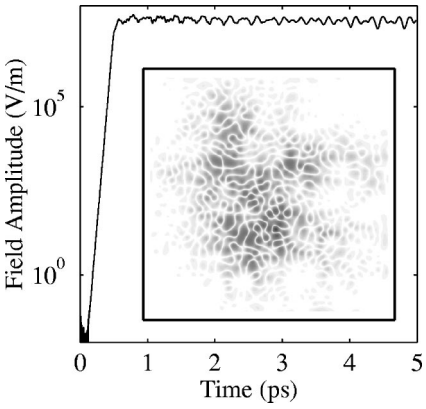

FIG. 12. Semilogarithmic representation of the field amplitude as a function of time recorded at an arbitrary location in the system, during the growth of the laser emission at a high pumping rate. The inset displays the spatial distribution of laser emission at an arbitrary time after the transient.

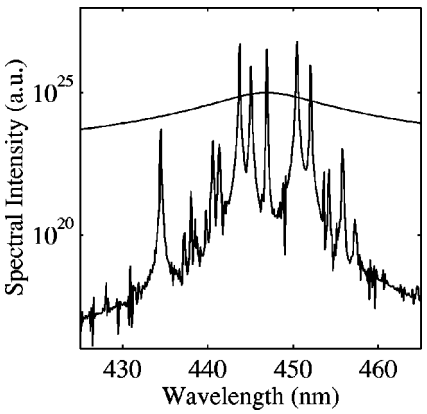

FIG. 13. Power spectrum of the laser field at high pumping rate, corresponding to the time record and the spatial map displayed in Fig. 12. The Lorentzian line shape of the gain is also shown.

nature of the localized modes. Since the modes are spatially localized and have different locations in the system, it is possible to pump the system locally instead of uniformly as in Sec. III B. The idea is to adjust the size and the location of the external pump in order to provide gain to a preferred mode and to prevent other modes from lasing.

For this purpose, we choose an external pump with a Gaussian spatial profile of width σ of the order of the localization length, $\sigma \approx \xi \approx 0.5$ μm. If its position is properly adjusted, it is possible to maximize the overlap of the gain with any localized mode. By scanning the system with the pump, we have been able to selectively excite each of the modes corresponding to the highest peaks of Fig. 5. We provide a few examples in the following.

A first example of local excitation is illustrated in Figs. 14 and 15. The circle in Fig. 15 indicates the location of the Gaussian pump, which has been located on purpose at the position of mode *e* (Fig. 6). Figure 14 displays the spatial distribution of the atomic population difference density

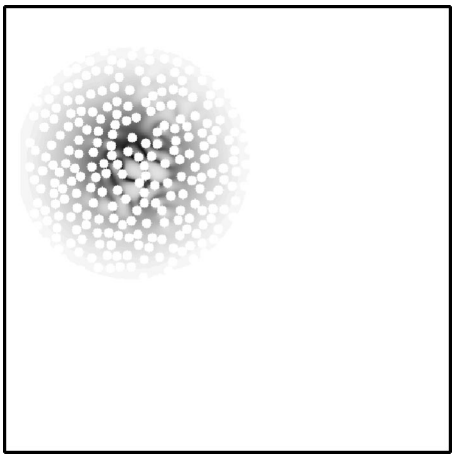

FIG. 14. Gray scale representation of the spatial distribution of the atomic population difference density ΔN between the upper and lower lasing levels for local excitation of the system by a Gaussian pump of width $\sigma = 0.5$ μm. The wide off-white spots inside the excited region indicate regions of gain saturation. The small white disks represent the scatterers in the same region.

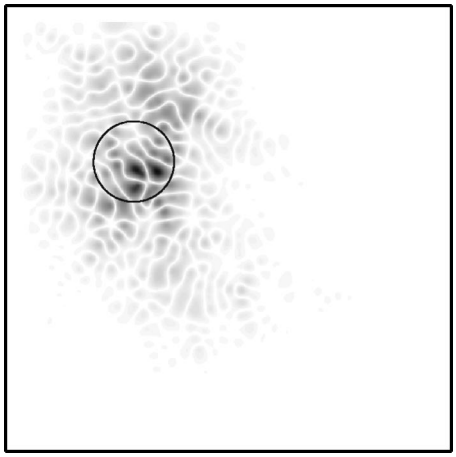

FIG. 15. Spatial distribution of the field amplitude of the laser emission for spatially localized gain. Compare with the spatial distribution of mode *e* in Fig. 6. The circle represents the spatial extension of the Gaussian pump at σ.

$-\Delta N = N_3 - N_2$ between the upper and lower levels of the laser transition. First, the population inversion is observed at the position of the external pump. Next, the saturation of the gain is also observed inside the active region as revealed by the spots where ΔN is strongly reduced (the wide off-white spots in Fig. 14). This is the well-known spatial hole burning effect occurring in our random laser as well as in conventional lasers.[33,35] The map of the laser mode that is excited in this case is shown in Fig. 15. One recognizes the map of mode *e* that is displayed in Fig. 6. The corresponding spectrum exhibits a unique peak at the eigenfrequency of mode *e* [Fig. 11(b)]. Once again, this example demonstrates that the modes of the passive random system act as ordinary modes of a conventional laser cavity. Moreover, although farther from the maximum $\lambda = 446.9$ nm of the gain curve and more dissipative than mode *b*, mode *e* has been excited alone. A second example is presented in Fig. 16 for the case where the external pump has a significant overlap with mode *d*. Comparison of Fig. 16 with Fig. 6 shows that mode *d* has been excited alone. The corresponding spectrum (not shown) once again exhibits a unique peak at the eigenfrequency of mode *d*. These results clearly illustrate the fact that the excited modes depend on the spatial location of the external pump. This is a distinctive property of random lasers, which has been observed in actual experiments.[11]

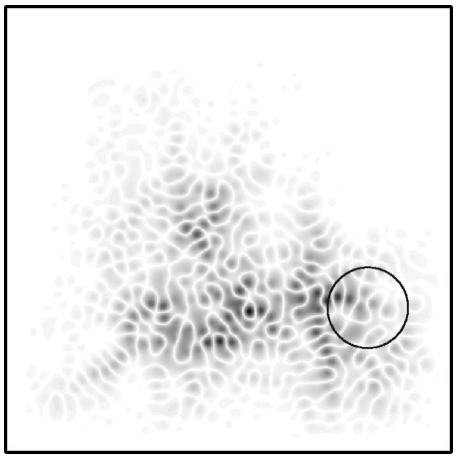

FIG. 16. Spatial distribution of the field amplitude of the laser emission for spatially localized gain. Compare with the spatial distribution of mode *d* in Fig. 6. The circle represents the spatial extension of the Gaussian pump at σ.

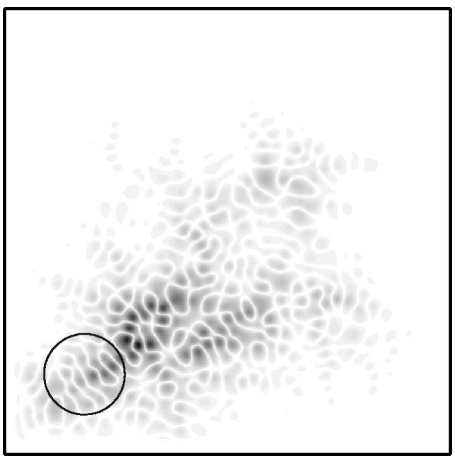

FIG. 17. Spatial distribution of the field amplitude of the laser emission for gain spatially localized near the boundaries of the system. The circle represents the spatial extension of the Gaussian pump at σ.

These examples demonstrate that it is possible to force the random laser to oscillate in a single mode different from mode *b*, which is the most favored one when the gain is extended. However, the modes that have been selected above are well localized inside the system and suffer reasonably low damping. One can ask what happens when the external pump is located near the boundaries of the system. This case is relevant for actual experiments since external pumping usually takes place in a thin layer, which corresponds to the penetration depth of the pump. Since leakage is important, the modes positioned at those locations are strongly damped. An example of local pumping near the boundaries of the

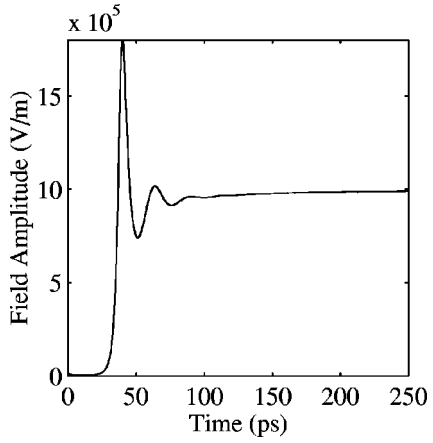

FIG. 18. Field amplitude as a function of time recorded at an arbitrary location in the system, during the growth of the laser emission for gain spatially localized near the boundaries of the system. The corresponding spatial map is displayed in Fig. 17.

system is presented in Fig. 17. Again, by adjusting the pumping rate just above threshold, a single mode is excited as demonstrated by the unique peak that characterizes the corresponding spectrum [Fig. 11(c)]. This spectrum and the map of the field amplitude displayed in Fig. 17 show that the excited mode is not one of the longest-lived modes that have been identified in the spectrum of the passive system (Fig. 5). The fact that this mode is strongly damped and has a short lifetime is reflected by relaxation oscillations during the transient buildup of the field when the laser is first turned on (Fig. 18).

IV. CONCLUSION

In summary, we have presented a numerical study of the interplay between Anderson localization and gain in a random laser. By considering the TM modes of a random array of parallel dielectric cylinders, we have first identified a range of parameters where such systems exhibit modes that are well localized with weak leakage through the boundaries. Laser gain has been introduced in the system by coupling Maxwell's equations with the rate equations of a four-level atomic system. The main result presented in this work demonstrates that the laser modes are identical to the modes of the passive system without gain. In other words, the modes of a random system behave as the cavity modes of a conventional laser. We have then considered the case where the external pumping is spatially localized. As observed in actual experiments, the excited modes of the random laser have been shown to depend on the location of the pump. In particular, by properly adjusting the position, the size and the rate of the external pump, it is possible to excite a single mode, which is different from the most favorable one. Even the strongly dissipative modes, which are located near the boundaries of the system, can be excited individually.

ACKNOWLEDGMENTS

We thank O. Legrand for a critical reading of the paper. This work has been supported by the Centre National de la Recherche Scientifique, the Research Group PRIMA and, the Direction Générale de l'Armement under Contract No. 0034041.

[1] V. S. Lethokov, Zh. Éksp. Teor. Fiz. **53,** 1442 (1967) [Sov. Phys. JETP **26**, 835 (1968)].
[2] C. Gouedart, D. Husson, C. Sauteret, F. Auzel, and A. Migus, J. Opt. Soc. Am. B **10**, 2358 (1993).
[3] P. Sebbah, D. Sornette, and C. Vanneste, in *OSA Proceedings on Advances in Optical Imaging and Photon Migration*, edited by R. R. Alfano (Optical Society of America, Washington, DC, 1994), Vol. 21, p. 68; P. Sebbah, Ph.D. Thesis, Université de Nice–Sophia Antipolis, France, 1993.
[4] N. M. Lawandy, R. M. Balachandra, A. S. L. Gomes, and E. Sauvain, Nature (London) **368**, 436 (1994).
[5] W. L. Sha, C. H. Liu, and R. R. Alfano, Opt. Lett. **19**, 1922 (1994).
[6] M. A. Noginov, H. J. Caulfield, N. E. Noginova, and P. Venkateswarlu, Opt. Commun. **118**, 430 (1995).
[7] D. S. Wiersma, M. P. van Albada, and A. Lagendijk, Phys. Rev. Lett. **75**, 1739 (1995).
[8] M. Siddique, R. R. Alfano, G. A. Berger, M. Kempe, and A. Z. Genack, Opt. Lett. **21**, 450 (1996).
[9] S. V. Frolov, Z. V. Vardeny, K. Yoshino, A. Zakhidov, and R. H. Baughman, Phys. Rev. B **59**, 5284 (1999).
[10] G. van Soest, M. Tomita, and A. Lagendijk, Opt. Lett. **24**, 306 (1999).
[11] H. Cao, Y. G. Zhao, H. C. Ong, S. T. Ho, J. Y. Dai, J. Y. Wu, and R. P. H. Chang, Appl. Phys. Lett. **73**, 3656 (1998); H. Cao, Y. G. Zhao, S. T. Ho, E. W. Seelig, Q. H. Wang, and R. P. H. Chang, Phys. Rev. Lett. **82**, 2278 (1999).
[12] H. Cao, Y. G. Zhao, H. C. Ong, and R. P. H. Chang, Phys. Rev. B **59**, 15107 (1999).
[13] D. S. Wiersma, M. P. van Albada, and A. Lagendijk, Nature (London) **373**, 203 (1995).
[14] H. Cao, J. Y. Xu, S.-H. Chang, and S. T. Ho, Phys. Rev. E **61**, 1985 (2000).
[15] S. John and G. Pang, Phys. Rev. A **54**, 3642 (1996).
[16] R. M. Balachandran and N. M. Lawandy, Opt. Lett. **21**, 1603 (1996).
[17] R. M. Balachandran, N. M. Lawandy, and J. A. Moon, Opt. Lett. **22**, 319 (1997).
[18] D. S. Wiersma and A. Lagendijk, Phys. Rev. E **54**, 4256 (1996).
[19] M. Kempe, G. A. Berger, and A. Z. Genack, in *Handbook of Optical Properties*, edited by R. E. Hummel and P. Wißmann (CRC Press, Boca Raton, FL, 1997), Vol. II, pp. 301–329.
[20] G. van Soest, F. J. Poelwijk, R. Sprik, and A. Lagendijk, Phys. Rev. Lett. **86**, 1522 (2001).
[21] H. Cao, J. Y. Xu, D. Z. Zhang, S.-H. Chang, S. T. Ho, E. W. Seelig, X. Liu, and R. P. H. Chang, Phys. Rev. Lett. **84**, 5584 (2000).
[22] X. Jiang and C. M. Soukoulis, Phys. Rev. Lett. **85**, 70 (2000).
[23] C. Vanneste and P. Sebbah, Phys. Rev. Lett. **87**, 183903 (2001).
[24] X. Jiang and C. M. Soukoulis, Phys. Rev. E **65**, 025601 (2002).
[25] C. M. Soukoulis, X. Jiang, J. Y. Xu, and H. Cao, Phys. Rev. B **65**, 041103 (2002).
[26] A. Taflove, *Computational Electrodynamics: The Finite-Difference Time-Domain Method* (Artech House, Norwood, MA, 1995).
[27] J. P. Berenger, J. Comput. Phys. **114**, 185 (1995).
[28] See P. C. de Oliveira, J. A. McGreevy, and N. M. Lawandy, Opt. Lett. **22**, 895 (1997); H. Cao, Y. G. Zhao, X. Liu, E. W. Seeling, and R. P. H. Chang, Appl. Phys. Lett. **75**, 1213 (1999) for an account of the experimental effect of external feedback on lasing in random media.
[29] See e.g., the discussion by B. Van Tiggelen in *Proceedings of the NATO Advanced Study Institute on Diffuse Waves in Complex*

Media, Les Houches, France, 1998, edited by J-P. Fouque (Kluwer, Dordrecht, 1999), p. 33, and references therein.
[30] E. Hoskinson and Z. Ye, Phys. Rev. Lett. **83**, 2734 (1999).
[31] A. A. Chabanov and A. Z. Genack, Phys. Rev. Lett. **87**, 153901 (2001).
[32] M. M. Sigalas, C. M. Soukoulis, C.-T. Chan, and D. Turner, Phys. Rev. B **53**, 8340 (1996).
[33] A. E. Siegman, *Lasers* (University Science Books, Mill Valley, CA, 1986).
[34] P. W. Milonni and J. H. Eberly, *Lasers* (Wiley, New York, 1988).
[35] M. Sargent, M. O. Scully, and W. E. Lamb, *Laser Physics* (Addison-Wesley, Reading, MA, 1982).